Design of thermal-anemometry-based probes for the simultaneous measurement of velocity and gas concentration in turbulent flows

Alaïs Hewes and Laurent Mydlarski

Department of Mechanical Engineering, McGill University, 817 Sherbrooke St. W., Montreal, QC H3A 0C3, Canada

E-mail: laurent.mydlarski@mcgill.ca

March 2021

Abstract.

Although thermal anemometry has been employed for the simultaneous measurement of velocity and gas concentration, the underlying theory and techniques to do so are not well established. To rectify this situation, the present work uses theory and experiments to investigate the design of thermal-anemometry-based probes capable of making such measurements, specifically focusing on those for use in helium/air mixtures. It is demonstrated that an interference probe, which consists of two hot-wires placed close enough together that one is located in the thermal wake of the other, can be used to simultaneously measure velocity and helium concentration. The performance of the probe is increased when (i) the separation distance (s) between the wires is small ($s/d_{up} \lesssim 2$, where d_{up} is the diameter of the upstream wire), and (ii) the downstream wire overheat ratio is low. Furthermore, a short downstream wire is recommended to ensure that the separation distance remains small while the wires are being operated.

Thermal-anemometry-based probes to measure velocity and concentration   2

1. Introduction

Thermal anemometry is a measurement technique which, owing to its (i) high spatial and temporal resolution, and (ii) high signal-to-noise ratio, remains one of the principal tools of turbulence research. As its name implies, this measurement technique uses the heat transfer from a heated sensor (either a fine wire or film) to infer the properties of the flow. Most commonly, a constant-temperature anemometer (i.e. one in which the sensor's temperature/resistance is maintained constant) is employed to measure the velocity of isothermal flows of homogeneous composition. Since the heat generated by passing an electric current through a sensor operated by such an anemometer is approximately equal to the heat convected away by the fluid flow, one finds that the output voltage of the anemometer (E) can be expressed as a function of the fluid velocity (U):

$$E^2 = A + BU^n, \tag{1}$$

in what is often referred to as King's Law‡. Although A and B are frequently treated as constants to be determined by calibration of the sensor in flows of known, constant velocity, it should be noted that both parameters are actually functions of the fluid temperature and composition:

$$A = 0.24\pi\Big(\frac{OH-1}{OH}\Big)\Big(\frac{T_f}{T}\Big)^{0.17}k\Big(\frac{1}{\alpha_{20}R_{20}}\Big)(R_T + R_L + R_w)^2 l, \tag{2}$$

$$B = 0.56\pi\Big(\frac{OH-1}{OH}\Big)\Big(\frac{T_f}{T}\Big)^{0.17}k\Big(\frac{\rho}{\mu}\Big)^n\Big(\frac{1}{\alpha_{20}R_{20}}\Big)(R_T + R_L + R_w)^2 l d^n. \tag{3}$$

Accordingly, as may be observed from the above equations, a constant-temperature anemometer can also be used to measure temperature or concentration of a chemical species. If multiple sensors are combined, simultaneous velocity and temperature or simultaneous velocity and concentration measurements are theoretically possible. Although techniques for the former are well established (see Bruun [1]), those for the latter are not.

2. Review of existing thermal-anemometry-based techniques for making simultaneous velocity and concentration measurements

Thermal-anemometry-based techniques for making simultaneous velocity and concentration measurements in fluid flows, or more specifically, the designs of probes capable of making such measurements, were primarily influenced by early theoretical work by Corrsin [2,3] and the experimental work of Way and Libby [4]. The former posited that the velocity and concentration fields of a turbulent flow could be inferred from the voltages of hot-wire probes of differing diameters (d). The latter were the first to implement these ideas, and designed a thermal-anemometry-based probe consisting of a hot-wire ($d_W = 2.5\,\mu$m) and hot-film ($d_F = 25\,\mu$m) to simultaneously measure velocity

‡ See Appendix A for a complete nomenclature and Appendix B for the full derivation of equation (1).

Thermal-anemometry-based probes to measure velocity and concentration   3

(U) and helium concentration (C). Initially, the hot-wire and hot-film were placed far enough apart that they could both be assumed to follow equation (1):

$$E_W^2 = A_W(C) + B_W(C)U^n, \tag{4a}$$
$$E_F^2 = A_F(C) + B_F(C)U^n, \tag{4b}$$

such that when eliminating the velocity from the above two equations, one obtains:

$$E_W^2 = A_W\left[1 - \left(\frac{B_W}{B_F}\right)\left(\frac{A_W}{A_F}\right)\right] + \left(\frac{B_W}{B_F}\right)E_F^2 = a(C) + b(C)E_F^2. \tag{5}$$

In theory, $a(C) \sim k$, and $b(C)$ is effectively independent of concentration. However, in their experiments, Way and Libby [4] found that *both* $a(C)$ and $b(C)$ were relatively weak functions of concentration, causing the hot-wire and hot-film to respond similarly to changes in U and C, and making it difficult to distinguish voltage pairs (E_W, E_F) measured in high concentration/low velocity flows from those measured in low concentration/high velocity flows. This was explained by the low thermal accommodation coefficient§ of helium on common hot-wire materials (i.e. tungsten, platinum), which causes thermal slip effects, and may affect the validity of the equations above. In contrast, when the hot-wire and hot-film were moved close enough together that their thermal fields "interfered," Way and Libby [4] discovered that sensitivity to concentration was sufficiently enhanced to make simultaneous velocity and concentration measurements possible.

Ultimately, Way and Libby [4] designed a probe (see table 1) in which the behavior of the hot-wire was strongly influenced by the hot-film's thermal field (due to the small separation distance between the two), but the latter was relatively unaffected by the presence of the hot-wire. The two sensors of this probe, which we refer to as an interference probe, therefore responded very differently to changes in the flow properties (i.e. U and C). For example, although the voltage measured across the hot-film was observed to increase with increasing helium concentration – as might be predicted from equations (1)-(3), or equation (4b) – the voltage measured by the hot-wire was nearly unaffected by concentration and, in some circumstances, even decreased with increasing helium concentration. This resulted from the fact that the thermal field of the hot-film expands as helium concentration increases (due to the increased thermal conductivity of this gas), which exposes the hot-wire to higher ambient temperatures, causing the voltage across it to decrease, and offsetting the expected increase from the increasing helium concentration. This distinct behavior made it possible to separate the effects of concentration from those of velocity, and unambiguously measure both fields.

§ The thermal accommodation coefficient relates to the energy transferred between a heated surface and colliding gas molecules. It is defined as the ratio of the average increase in energy of the molecules after striking the surface to the increase in energy if the molecules were to have time to come into thermal equilibrium with the surface (i.e. the maximum possible energy increase based on thermodynamics). It is bound between 0, when no energy is transferred from the surface, and 1, when the surface and gas molecules are in thermal equilibrium.

Thermal-anemometry-based probes to measure velocity and concentration

Table 1: Summary of the designs of previously developed thermal-anemometry-based probes for the simultaneous measurement of velocity and concentration. The gas mixture in which the probes were used is provided. The sensors (upstream and downstream, if the orientations are specified) are described in terms of their diameter and, if available, the wire/film material (tungsten - W; platinum - Pt; platinum-rhodium - Pt/Rh). All probes with separation distances (s) of less than 50 μm (such that $s/d_{hot} \leq 10$) have been classified as interference probes.

Reference	Gas Mixture	Upstream Sensor / Sensor 1	Downstream Sensor / Sensor 2	Diameter Ratio	Separation Distance (μm)	$OH_{up/1}$ or $T_{w,up/1}$ (°C)	$OH_{down/2}$ or $T_{w,down/2}$ (°C)	Angle Btwn. Sensors	Interference Probe
Way and Libby [4]	He/air $0 \leq C \leq 0.35$	2.5 μm Pt wire	25 μm Pt film	10	50	~ 120°C	~ 295°C	90°	Yes
Way and Libby [8]	He/air $0 \leq C \leq 0.35$	2.5 μm Pt wire	25 μm Quartz-coated Pt film	10	25	~ 145°C	~ 320°C	90°	Yes
McQuaid and Wright [9]	Ar/air $0 \leq C \leq 1.0$	2.5 μm Pt wire	10 μm Pt wire	4.0	N/A	1.3	2.5	N/A	No
Stanford and Libby [10] LaRue and Libby [11,12][1]	He/air $0 \leq C \leq 1.0$	2.5 μm W wire	25 μm film	10	25	85°C	305°C	30°	Yes
Sirivat and Warhaft [13]	He/air $0 \leq C < 0.02$	5 μm Pt/Rh wire	3 μm W wire	1.7	5	1.6	1.2	10°	Yes
Panchapakesan and Lumley [14][1]	He/air $0 \leq C \leq 0.06$	9 μm W wire	3 μm W wire	3.0	5	1.8	1.6	Nearly parallel	Yes
Harion and co-workers [5,6,15,16], Soudani and Bessaïh [17,18]	He/air $0 \leq C \leq 1.0$	2.5 μm wire	70 μm film	28	25	250°C	100°C	90°	Yes
Sakai et al. [19]	CO$_2$/air $0 \leq C \leq 1.0$	5 μm W wire	5 μm Pt wire	1.0	500	1.3	2.4	Parallel	No
Jonàš et al. [20], Mazur et al. [21]	He/air $0 \leq C \leq 1.0$	5 μm W wire	70 μm film	14	1000	$187 - 250$°C	$77 - 100$°C	90°	No

[1] Probe is combined with other thermal-anemometry-based sensors (hot-wires, hot-films) to measure two components of the velocity field and concentration

Thermal-anemometry-based probes to measure velocity and concentration   5

As may be observed in table 1, most subsequent thermal-anemometry-based probes for the simultaneous measurement of velocity and gas concentration‖ are based on the work of Way and Libby [4]; they consist of two sensors (hot-wires, hot-films) placed within 50 μm of each other, such that $s/d_{hot} \leq 10$ (where s is the separation distance, and d_{hot} is the diameter of the hottest sensor of the probe) and some thermal interference between the sensors is therefore likely. However, given that the diameter ratio of these probes is generally large, Corrsin's [2,3] earlier suggestion – that simultaneous velocity and concentration measurements can be achieved using hot-wires with differing diameters – continues to influence the design of probes used to make such measurements. This suggestion has been reiterated by Harion et al. [5], Soudani et al. [6], and McQuaid and Wright [7], although it should be noted that, similarly to Corrsin [2,3], their arguments were (i) primarily theoretical and (ii) limited to non-interfering probes (i.e. probes in which the sensing elements were placed far enough apart that their thermal fields would not interact). Moreover, neither Corrsin [2,3] nor McQuaid and Wright [7] considered the effects of thermal-slip (which may be significant in flows of helium). Thus, the relevance of the suggestions given in the aforementioned works to most of the probes presented in table 1 is not particularly clear and merits further investigation.

In general, there has been relatively little work investigating the design of thermal-anemometry-based probes capable of simultaneously measuring velocity and gas concentration. Given a thorough review of the designs of such probes (which are all compiled in table 1), the following can be inferred:

(i) As stated above, a large diameter ratio *may* be beneficial [2,3,5–7]. However, large diameter ratios often require the use of a hot-film, which has a poor frequency response compared to a hot-wire. Accordingly, to improve the temporal and spatial resolution of the thermal-anemometry-based probe, it should ideally be composed of two hot-wires, like in the work of McQuaid and Wright [9], Sirivat and Warhaft [13], Panchapakesan and Lumley [14], and Sakai et al. [19].

(ii) Probes with separation distances small enough that thermal interference effects are likely ($s/d_{hot} \leq 10$), which herein are referred to as interference probes, appear to be necessary in He/air mixtures. For most of these probes, s/d_{hot} is approximately 1 or 2, but Harion et al. [5] (and related works [6,15–18]), designed a probe in which $s/d_{hot} = 10$, and in which interference effects were considered to be of secondary importance due to the large diameter ratio of the sensing elements. Interference probes do not appear to be necessary in other gas mixtures, as evidenced by the work of McQuaid and Wright [9] and Sakai et al. [19].

(iii) Differences in the overheat ratios of the sensors, or, more generally, their operating temperatures, can be observed for each of the probes listed in table 1. In non-interfering probes, these differences can be used to increase sensitivity

‖ Note that we consider only the simplest of these probes, which are specifically used to make simultaneous measurements of a single component of velocity and concentration when the mean flow direction is known.

to concentration [7] and/or make simultaneous-velocity and concentration measurements possible [19]. In CO_2/air mixtures, a difference in the overheat ratio is all that is required for making such measurements [19]. When using interference probes, differences in overheat ratios can be used to control the degree to which one sensing element of the probe is affected by the thermal field of the other [5, 6].

Although the above statements lend some insight into the design of thermal-anemometry-based probes used to simultaneously measure velocity and gas concentration, they do not reveal the necessary or optimal design parameters required to construct or operate such probes. Adapting, improving, or even recreating these thermal-anemometry-based probes for specific experimental situations is therefore difficult. To rectify this situation, the present work investigates in greater detail the design of thermal-anemometry-based probes capable of simultaneously measuring velocity and concentration in turbulent flows.

The remainder of this paper is organized as follows. §3 further develops the theory underlying the use of thermal anemometry for making simultaneous velocity and gas concentration measurements in fluid flows. Then, in §4, we present the details and results of an experimental investigation into the design of thermal-anemometry-based probes capable of making measurements in He/air mixtures. The present work specifically focuses on such probes since (i) helium is generally an attractive gas for studying flows of heterogeneous mixtures (as it is inert, non-toxic, and relatively inexpensive), and (ii) its relatively low density and Schmidt number makes it useful for studying variable-density flows (as is the case for many of the works cited in table 1 [8, 10–12, 14–18]) or differential diffusion. Finally, the conclusions and future work are discussed in §5.

3. Theory

Since thermal-anemometry-based probes that use a hot-film have a poor frequency response, the present work only focuses on probes consisting of a pair of hot-wires. The theoretical anaysis presented herein therefore begins by considering how two hot-wires can be used to make simultaneous velocity and concentration measurements in any gas mixture.

3.1. Thermal-anemometry-based probes capable of simultaneously measuring velocity and concentration in any gas mixture

Following the approach of Way and Libby [4], we first consider the case in which two wires are placed side-by-side and far enough apart that their thermal fields do not interfere. In this situation, both wires follow equation (1) (King's Law). Accordingly, the wire voltages (E_1, E_2) can be expressed as a function of each other, independent of the fluid velocity (U):

$$E_2^2 = a(C) + b(C)E_1^2. \tag{6}$$

Thermal-anemometry-based probes to measure velocity and concentration   7

To obtain simultaneous velocity and concentration measurements, a and/or b must be functions of concentration (C), so that distinct iso-concentration curves for E_2 as a function of E_1 can be obtained in the E_2-E_1 plane. Using the definitions of A and B provided in equations (2) and (3), $a(C)$ and $b(C)$ can be expressed as:

$$a(C) = 0.24\pi \left(\frac{OH_2 - 1}{OH_2}\right)\left(\frac{T_{f,2}}{T}\right)^{0.17} k_2(R_{T,2} + R_{L,2} + OH_2 R_{a,2})$$
$$\left(\frac{l_2}{\alpha_{20,2}R_{20,2}}\right)\left[1 - \left(\frac{\rho_2}{\rho_1}\frac{\mu_1}{\mu_2}\right)^n\left(\frac{d_2}{d_1}\right)^n\right], \tag{7}$$

$$b(C) = \left[\frac{(OH_2 - 1)/OH_2}{(OH_1 - 1)/OH_1}\right]\left(\frac{T_{f,2}}{T_{f,1}}\right)^{0.17}\frac{k_2}{k_1}\left(\frac{\rho_2}{\rho_1}\frac{\mu_1}{\mu_2}\right)^n$$
$$\left[\frac{R_{T,2} + R_{L,2} + OH_2 R_{a,2}}{R_{T,1} + R_{L,1} + OH_1 R_{a,1}}\right]\left(\frac{\alpha_{20,1}R_{20,1}}{\alpha_{20,2}R_{20,2}}\right)\left(\frac{l_2}{l_1}\right)\left(\frac{d_2}{d_1}\right)^n. \tag{8}$$

As may be observed from the above equations, b is generally a weak function of concentration, and becomes independent of concentration for the specific case in which the wire temperatures are equal (so that $T_{f,1} = T_{f,2}$, $k_1 = k_2$, $\mu_1 = \mu_2$, $\rho_1 = \rho_2$). Accordingly, a must therefore be a function of concentration (and non-zero) to concurrently measure velocity and concentration, which necessitates that:

$$\left(\frac{\rho_2}{\rho_1}\frac{\mu_1}{\mu_2}\right)^n\left(\frac{d_2}{d_1}\right)^n \neq 1. \tag{9}$$

Consequently, simultaneous measurements of velocity and concentration are theoretically possible if (i) $d_1 \neq d_2$, or (ii) $T_{f,1} \neq T_{f,2}$.

Although the above analysis is consistent with previous work suggesting that thermal-anemometry-based probes capable of simultaneous measurements of velocity and concentration be designed to have large diameter ratios [2, 3, 5–7], it also demonstrates that differences in the wire diameter are not a necessary condition. Like in the work of Sakai et al. [19], it should be possible to design such probes that consist of two hot-wires operated at two different overheat ratios. Nevertheless, this depends significantly on the choice of gas-mixture. Given the focus of the present work on the design of probes capable of making measurements in He/air mixtures (like most of the probes presented in table 1), it is worth discussing the theory behind making such measurements in greater detail.

3.2. Thermal-anemometry-based probes capable of simultaneously measuring velocity and concentration in He/air mixtures

The simultaneous measurement of velocity and helium concentration requires an understanding of thermal slip, which may be caused by rarified gas and/or accommodation effects, and which can be relevant to He/air mixtures. Rarified gas effects may be quantified by the Knudsen number ($\text{Kn} \equiv \lambda/d$), which increases with the concentration of helium (in helium/air mixtures). As the Knudsen number increases, the flow over a hot-wire may transition from continuum flow to slip flow, resulting

Thermal-anemometry-based probes to measure velocity and concentration   8

in a decrease of the expected Nusselt number of the wire [22, 23]. Moreover, thermal slip can even occur in what is normally considered continuum flow (Kn < 0.01) if the accommodation coefficient (α) for the gas on the wire is small [24–26]. Although accommodation coefficients are near-unity for most common gases (including air) on hot-wire materials [23, 27], they are relatively small for helium, with quoted values ranging from $0.03 - 0.48$ [25–27]. With both high Knudsen numbers and low accommodation coefficients, thermal slip is likely in flows containing helium, and the actual heat transfer from the hot-wire is expected to be lower than what is predicted from equations (1)-(3).

To take into account rarified gas and accommodation effects, we suggest that equations (1)-(3) be replaced with the following equation, derived in Appendix C from the work of Collis and Williams [22] and Andrews et al. [23]:

$$E^2 = \pi \Big(\frac{OH - 1}{OH}\Big) k \Big(\frac{l}{\alpha_{20} R_{20}}\Big)(R_T + R_L + R_w)^2 \frac{\mathrm{Nu}_c}{1 + \mathrm{Nu}_c \Phi \mathrm{Kn}}, \tag{10}$$

where Nu_c is the continuum Nusselt number predicted by the heat transfer correlation of Collis and Williams [22], and Φ is a function of the accommodation coefficient ($\Phi = f(\alpha)$). However, due to the large uncertainty surrounding values of α, it is important to note that the above equation may only estimate these effects.

Nevertheless, we can use equation (10) to gain further insight into the design of thermal-anemometry-based probes capable of simultaneously measuring velocity and concentration in He/air mixtures. In the present work, we calculated the theoretical voltages (E_1, E_2) of two select configurations of commercially available hot-wires (1.2 μm Pt and 10 μm W; 2.5 μm W and 2.5 μm Pt/Rh) over the range of conditions corresponding to the experimental data presented in §4 ($1\,\mathrm{m/s} \leq U \leq 15\,\mathrm{m/s}$, $0 \leq C \leq 0.06$), and plotted the results in figures 1 and 2. Given that figures 1 and 2 respectively depict the theoretical response of a probe designed with a (i) large diameter ratio ($d_2/d_1 = 8.3$) and (ii) large wire/film temperature differences ($T_{w,2} - T_{w,1} = 486$°C; $T_{f,2} - T_{f,1} = 243$°C), we can assess whether our earlier conclusions – that simultaneous velocity and concentration measurements are possible if $d_1 \neq d_2$ or $T_{f,1} \neq T_{f,2}$ – are valid in He/air mixtures.

To highlight the importance of rarified gas and accommodation effects in He/air mixtures, both figures 1 and 2 compare the behavior of a hot-wire predicted by equations (1)-(3) (which do not correct for rarified gas and accommodation effects, and from which equations (7) and (8) are derived) and equation (10) (which takes into account rarified gas and accommodation effects). Consistent with the theory presented in §3.1, equations (1)-(3) predict distinct iso-concentration curves for the probe depicted in figure 1 ($d_2/d_1 = 8.3$). However, for that same probe, when rarified and accommodation effects are taken into account, the iso-concentration curves collapse onto a single line, such that simultaneous measurement of velocity and concentration is not possible. This agrees well with experimental data presented by Way and Libby [4] for a probe with a similar diameter ratio ($d_F/d_W = 10$), and suggests that Way and Libby [4] were indeed correct in assuming that thermal slip caused their experimental data to deviate from theoretical predictions (see equations (4a), (4b), and (5)). In the case of the probe

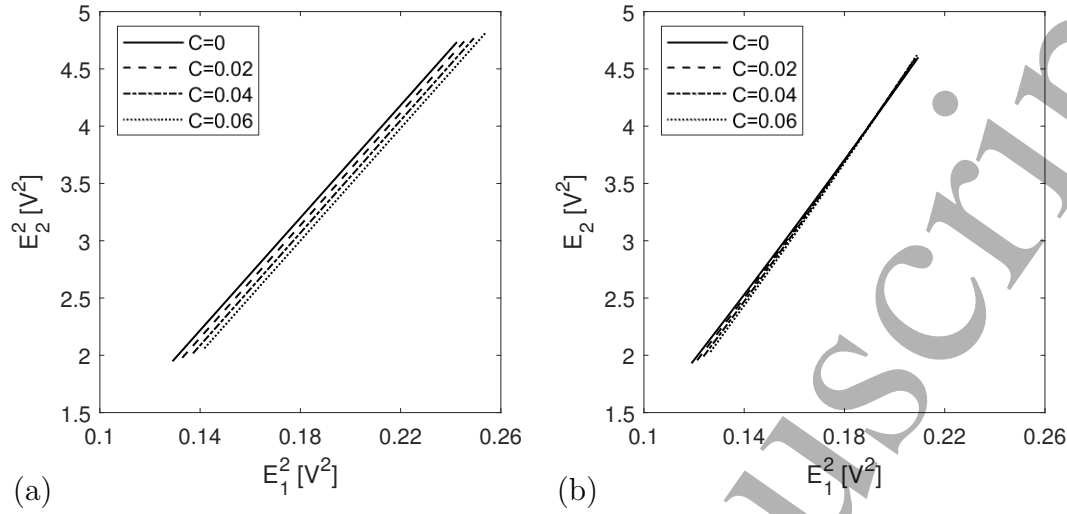*Thermal-anemometry-based probes to measure velocity and concentration*   9

Figure 1: Theoretical dependence of E_2^2 on E_1^2 using (a) equations (1)-(3), and (b) equation (10). The first wire is made of platinum ($d_1 = 1.2\,\mu$m) and the second wire is made of tungsten ($d_2 = 10\,\mu$m). Both are operated at $OH = 1.8$.
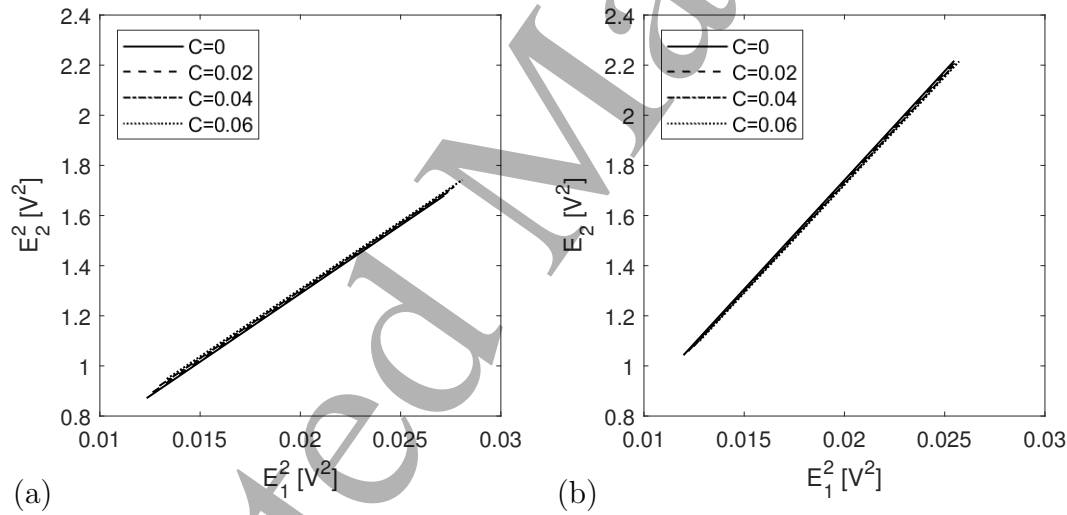

Figure 2: Theoretical dependence of E_2^2 on E_1^2 using (a) equations (1)-(3), and (b) equation (10). The first wire is made of tungsten and operated at $OH = 1.05$ ($T_{w,1} = 34$°C; $T_{f,1} = 27$°C) and the second wire is made of platinum-rhodium and operated at $OH = 1.8$ ($T_{w,2} = 520$°C; $T_{f,2} = 270$°C). Both are 2.5 μm in diameter.

analyzed in figure 2 ($T_{w,2} - T_{w,1} = 486$°C; $T_{f,2} - T_{f,1} = 243$°C), both equations (1)-(3) and equation (10) demonstrate that the iso-concentration curves all collapse onto each other, and simultaneous velocity and concentration measurement are, once again, impossible.

Based on the above analysis, it can be concluded that for the range of helium concentrations of interest, neither a large diameter ratio ($d_2/d_1 = 8.3$), nor an extremely large wire/film temperature difference ($T_{w,2} - T_{w,1} = 486$°C; $T_{f,2} - T_{f,1} = 243$°C), are sufficient for making simultaneous velocity and concentration measurements, despite what was inferred earlier from equations (7) and (8). Not only

Thermal-anemometry-based probes to measure velocity and concentration 10

are the theoretical thermal-anemometry-based probes nearly insensitive to differences in wire/film temperatures, but rarified gas and accommodation effects in He/air mixtures have a significant effect on these probes, and render imperceptible any changes that could be attributed to differences in wire diameters. Accordingly, the design recommendations put forth by Corrsin [2, 3], Harion et al. [5], Soudani et al. [6], and McQuaid and Wright [7] do not appear to be well suited to flows containing helium mixtures.

3.3. Interference probes in He/air mixtures

It is worth pointing out that the diameter ratio of the hot-wires investigated in figure 1 was chosen to be as large as realistically possible, and cannot be increased significantly beyond its current value (since the dimensions of the wires are limited due to end conduction effects, spatial resolution requirements, and CTA specifications). Given the results presented in figures 1 and 2, and practical constraints for hot-wire designs, it appears that the only possible way to increase sensitivity to helium concentration is to bring the wires of the probe close enough together that one is in the thermal wake of the other, thus forming an interference probe, like in the work of Way and Libby [4]. The behavior of such a probe is complex and cannot be predicted using the equations presented in the current section, which were derived assuming that the probe wires are placed sufficiently far apart that their thermal fields do not interfere. To gain insight into the physics of interference probes, and understand how to design these probes, we therefore undertake an experimental investigation.

4. Experimental investigation on the design of interference probes capable of simultaneously measuring velocity and helium concentration

4.1. Details of interference probes studied

To study the design of interference probes capable of simultaneously measuring velocity and helium concentration, we constructed and tested 21 different probes of varying designs, the details of which are given in table 2. The interference probes were all built by hand using the techniques described in Hewes [28], and mounted on modified TSI 1240 X-wire probes, as depicted in figure 3. They are described using abbreviations pertaining to the upstream wire diameter and material, downstream wire diameter and material, and separation distance (e.g. 2.5W-2.5W-10, 10W-5W-10, 2.5W-1.2Pt-35, etc.).

It is important to note that possible designs for these interference probes were limited by constraints on which types of hot-wires could be used (e.g. commercially available wires, spatial resolution requirements, CTA specifications), and our ability to construct the probe. Creating the probes was very delicate work, as each required that $1.2 - 10$ micron-diameter wires be separated by a distance on the order of tens of microns. Nevertheless, a large number of probes with different designs have been investigated, lending insight into the effect that three important parameters of interest

Thermal-anemometry-based probes to measure velocity and concentration 11

Table 2: Summary of interference probes designed for the present work. The diameter (in μm) and wire material (tungsten - W, platinum - Pt, platinum-rhodium - Pt/Rh) of the upstream and downstream wire is provided, as is the diameter ratio (d_{up}/d_{down}), wire separation distance (s), and range of lengths of the upstream and downstream wires (l_{up}, l_{down}).

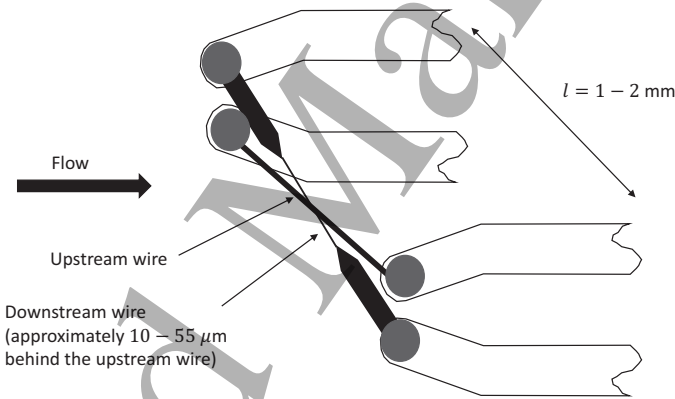| Upstream Wire	Downstream Wire	d_{up}/d_{down}	s (μm)	l_{up} (mm)	l_{down} (mm)
2.5 W	2.5 W	1	10, 25, 55	$0.7 - 1.4$	$0.3 - 1.2$
5 W	5 W	1	10, 10	$1.5 - 2.7$	0.5
2.5 W	1.2 Pt	2	35	0.9	0.4
5 W	2.5 W	2	10, 20	$1.1 - 2.2$	$0.2 - 1.4$
5 W	2.5 Pt/Rh	2	10, 10, 10, 15, 15	$2.2 - 2.5$	$0.2 - 0.5$
10 W	5 W	2	10, 10, 10, 15, 25	2.3	$0.5 - 1.0$
10 W	2.5 W	4	25, 25, 35	$2.3 - 2.6$	$0.5 - 1.5$

Figure 3: Schematic representation of an interference probe mounted on a modified TSI 1240 X-wire probe. Note that the prongs are bent, so that the wires cross at an angle of $20 - 30°$. This helps ensure that a large potion of the downstream wire is located within the thermal wake of the upstream wire.

– the diameter ratio, separation distance between the wires, and overheat ratio – have on the performance of an interference probe.

4.2. Experimental apparatus

The interference probes were calibrated and tested using a commercially produced TSI Model 1128B Air Velocity Calibrator, which generates an effectively laminar, uniform, velocity profile at its 1cm diameter (D) exit nozzle. He/air mixtures were produced far upstream of this calibration jet by joining a continuous stream of air with a continuous stream of helium, as depicted in figure 4. The length of tubing following the T-junction at which the gas flows merge exceeded 400 diameters, and accordingly allowed both gases to mix fully before reaching the calibration jet. The flow rate of the air was set

Thermal-anemometry-based probes to measure velocity and concentration   12

with a needle valve and measured with a 100 slpm mass flow meter (Alicat M-100SLPM-D), and the flow rate of helium was measured and controlled with a 20 slpm mass flow controller (Alicat MC-20SLPM-D). An automated, custom-made LabVIEW program was used to set the flow rate of helium and maintain constant helium concentrations during calibrations and experiments. Additional details pertaining to this apparatus, including relevant uncertainties, can be found in Hewes [28, 29].
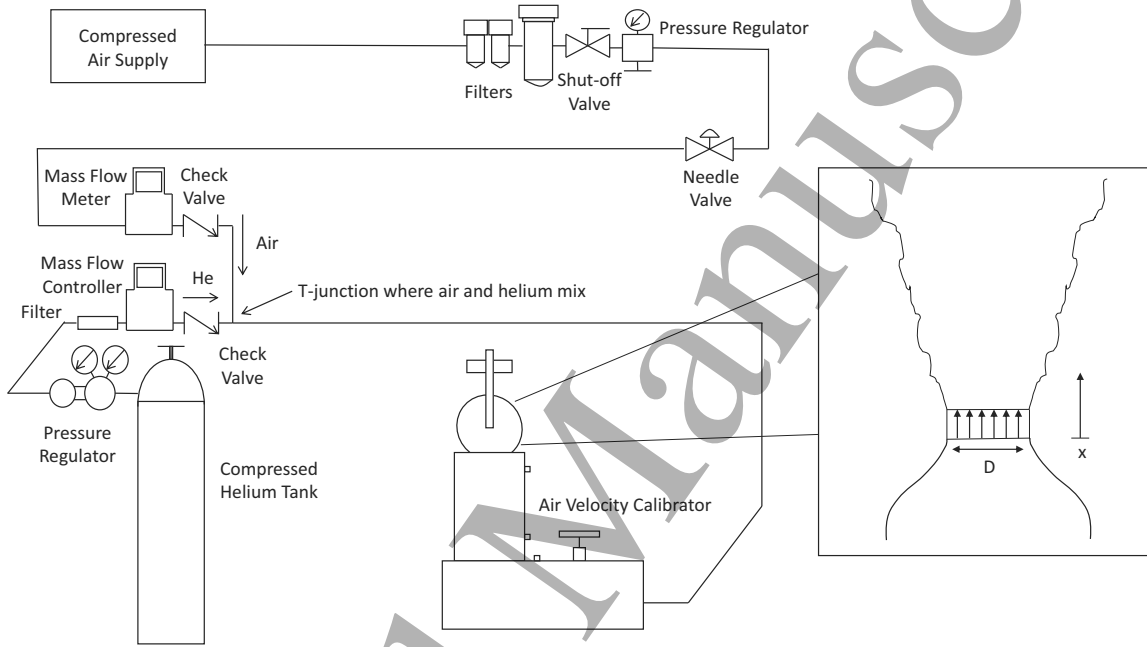

Figure 4: Schematic of the experimental apparatus.

The probes presented in table 2 were calibrated at the exit of the calibration jet, where the flow is laminar and uniform. Actual experiments were performed in the jet, at a distance of $x/D = 10$ from the jet exit, where the flow is fully turbulent. The probes were all operated using two channels of a TSI IFA300 Constant Temperature Anemometer and digitized using a 16-bit National Instrument PCI-6143 data acquisition board that was controlled by a second custom-made LabVIEW program. During the experiments, the signals from each of the probe's wires were band-pass filtered using a Krohn-Hite 3384 filter, and, if necessary, amplified. Time series of the data were typically obtained by sampling 3.3×10^7 points at twice the low-pass frequency (20 kHz, since the low-pass frequency was generally set to 10 kHz).

4.3. Calibration

Calibrations were generally performed for velocities in the range $1 \lesssim U \lesssim 13$ m/s and concentrations (in terms of the helium mass fraction) of 0, 0.02, 0.04, and 0.06. The voltages of both wires were recorded for each velocity and concentration, forming a calibration map like the one shown in figure 5. As noted in §3, simultaneous velocity and

Thermal-anemometry-based probes to measure velocity and concentration   13

concentration measurements are only possible when distinct iso-concentration curves can be identified (as is the case for the probe used for figure 5).
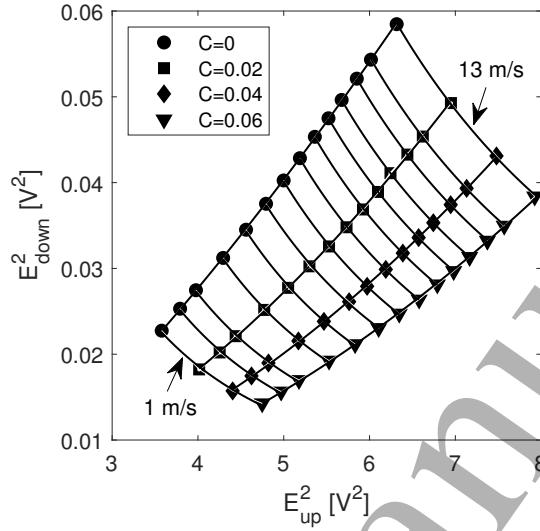

Figure 5: Calibration map for an interference probe consisting of a $10\,\mu$m diameter tungsten wire placed $10\,\mu$m upstream of a $5\,\mu$m diameter tungsten wire (10W-5W-10). The squared voltage of the downstream wire is plotted as a function of the squared voltage of the upstream wire for velocities ranging from 1 to 13 m/s and concentrations of 0, 0.02, 0.04, and 0.06 He mass fraction. Power laws are fit to the data along iso-concentration and iso-velocity lines.

The overheat ratios at which the wires were operated were observed to have a significant effect on the shape of the calibration map. Two examples are presented demonstrating this. The first involves a probe consisting of a $2.5\,\mu$m diameter tungsten wire placed $35\,\mu$m upstream of a $1.2\,\mu$m diameter platinum wire (2.5W-1.2Pt-35) and the second involves a probe consisting of a $10\,\mu$m diameter tungsten wire placed $10\,\mu$m upstream of a $5\,\mu$m diameter tungsten wire (10W-5W-10). Both probes were calibrated with:

 (i) both wires operated at overheat ratios of 1.8,

(ii) the upstream wire operated at an overheat ratio of 1.8 and the downstream wire operated an overheat ratio of 1.2,

(iii) the upstream wire operated at an overheat ratio of 1.2 and the downstream wire operated at an overheat ratio of 1.8, and

(iv) both wires operated at overheat ratios of 1.2.

As demonstrated in figures 6 and 7, the calibration maps for each combination of overheat ratios are quite different. Similar results were obtained by Harion et al. [5], who also studied the effect of overheat ratios (i.e. sensor temperature) on an interference probe consisting of a hot-wire and hot-film. They found that the choice of sensor temperatures could be used to design probes in which (i) neither sensor was significantly influenced by the thermal field of the other, (ii) the hot-film was influenced by the

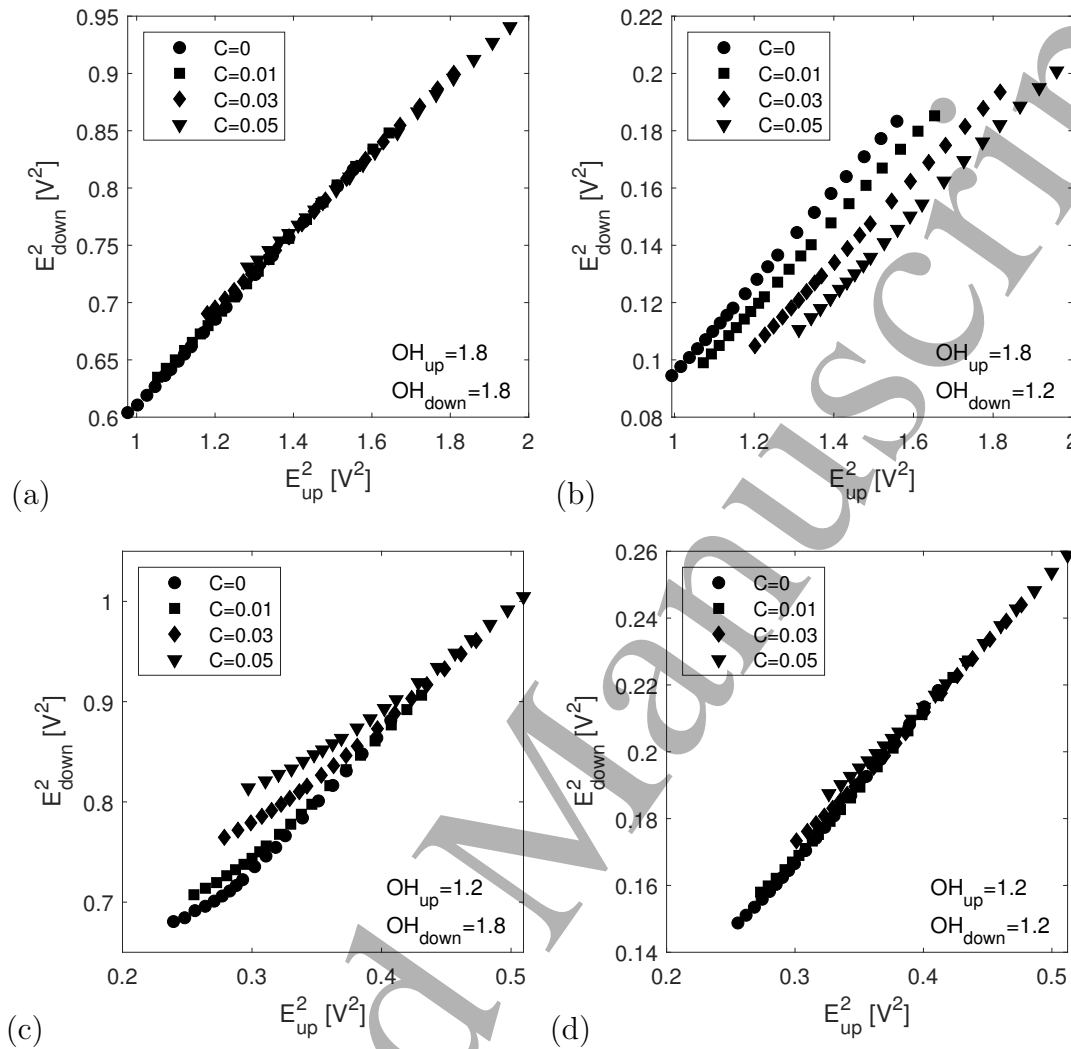*Thermal-anemometry-based probes to measure velocity and concentration* 14

Figure 6: Comparison of the effects of the overheat ratio on the calibration map of the 2.5W-1.2Pt-35 probe. (a) Upstream wire $OH = 1.8$ and downstream wire $OH = 1.8$. (b) Upstream wire $OH = 1.8$ and downstream wire $OH = 1.2$. (c) Upstream wire $OH = 1.2$ and downstream wire $OH = 1.8$. (d) Upstream wire $OH = 1.2$ and downstream wire $OH = 1.2$.

thermal field of the hot-wire, and (iii) the hot-wire was influenced by the thermal field of the hot-film. In the current work, it appears that sensitivity to concentration is enhanced when the (smaller) downstream wire is operated at a low overheat ratio and the (larger) upstream wire is operated at a high overheat ratio, such that the former is influenced by the thermal field of the latter. This is especially apparent for the 2.5W-1.2Pt-35 probe (figure 6), for which simultaneous velocity and concentration measurements are only possible when the upstream wire overheat ratio is high and the downstream wire overheat ratio is low. Consequently, the interference probes used herein were all operated with the aforementioned combination of overheat ratios. Differences between the calibration maps of the 2.5W-1.2Pt-35 probe (figure 6) and those of the 10W-5W-10 probe (figure 7) are most likely due to differences in the separation distance between

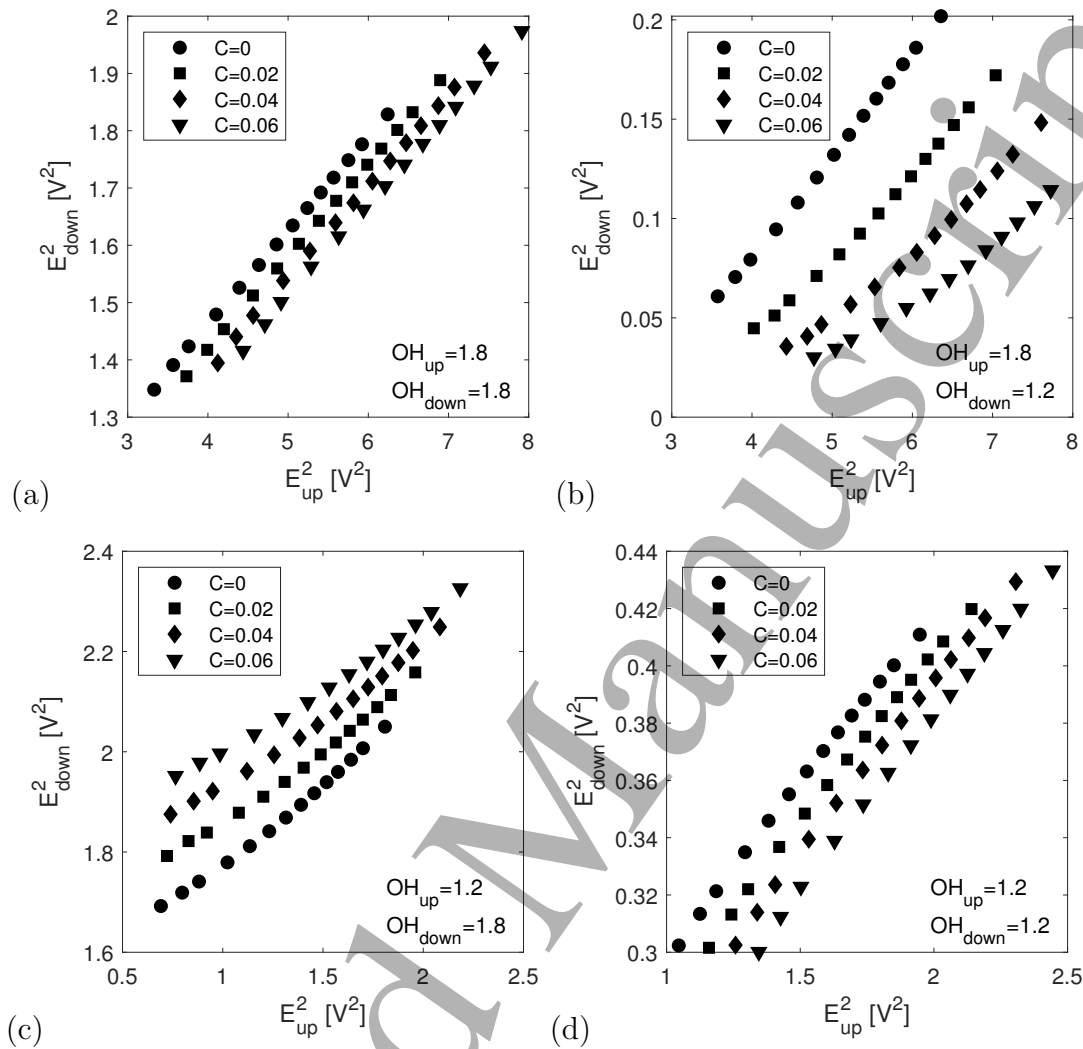*Thermal-anemometry-based probes to measure velocity and concentration* 15

Figure 7: Comparison of the effects of the overheat ratio on the calibration map of the 10W-5W-10 probe. (a) Upstream wire $OH = 1.8$ and downstream wire $OH = 1.8$. (b) Upstream wire $OH = 1.8$ and downstream wire $OH = 1.2$. (c) Upstream wire $OH = 1.2$ and downstream wire $OH = 1.8$. (d) Upstream wire $OH = 1.2$ and downstream wire $OH = 1.2$.

the two wires of the probes. Since the wires of the 10W-5W-10 probe are much closer together, simultaneous velocity and concentration measurements are possible for each combination of overheat ratios. The effects of separation distance, as well as other design parameters, are investigated in greater detail in §4.6. However, the data reduction and validation measurements for the interference probe are presented first.

4.4. Data reduction

To calculate the concentration from the output voltages of the anemometers, a two-dimensional fit of the following form can be applied to the calibration map of the two

Thermal-anemometry-based probes to measure velocity and concentration   16

wire voltages of an interference probe (E_{up}, E_{down}):

$$C = c_1(\ln E_{up}^2)^3 + c_2(\ln E_{down}^2)^3 + c_3(\ln E_{up}^2)^2 \ln E_{down}^2 +$$
$$c_4 \ln E_{up}^2(\ln E_{down}^2)^2 + c_5 \ln E_{up}^2 \ln E_{down}^2 + c_6(\ln E_{up}^2)^2 + \qquad (11)$$
$$c_7(\ln E_{down}^2)^2 \ln + c_8 \ln E_{up}^2 + c_9 \ln E_{down}^2 + c_{10}$$

Although polynomial fits were suggested in earlier works [13, 28], analysis of different curve fits revealed that the fit at low velocities was improved when using logarithms of the voltages instead. Moreover, as may be observed in figure 5, which is representative of most calibration maps, the iso-concentration and iso-velocity curves each exhibit power-law behaviors, which suggests that a fit of the form of equation (11) is more representative of the relationship between C, E_{up}, E_{down} than a two-dimensional polynomial fit.

The velocity can then be obtained by applying an inversion of equation (1) to the upstream wire:

$$U = \left[\frac{E_{up}^2 - A(C)}{B(C)}\right]^{1/n}. \qquad (12)$$

The functions $A(C)$ and $B(C)$ in the equation above are determined by fitting equation (1) to iso-concentration curves of the upstream wire, as shown in figure 8(a). The values of A and B obtained from each of the iso-concentration curves are then plotted as a function of C, as depicted in figures 8(b) and (c). Using this process, which resembles that used when calibrating a hot-wire in non-isothermal flows (described in Bruun [1] and Berajeklian [30], and employed to make simultaneous velocity and temperature measurements in Berajeklian amd Mydlarski [31], for example), one finds that $A(C)$ and $B(C)$ can be well approximated by second-order polynomial functions of C.

Assuming that no drift (resulting from changes in the ambient temperature and/or wire aging [32]) occurs after the wires are calibrated, the above data reduction scheme can be used to infer the velocity and concentration at each point in the flow from the measured voltages of both wires (E_{up}, E_{down}). First, equation (11) is used to calculate C, and then, using that value of C, equation (12) is used to calculate U. The calculated values of U and C deviate from their true values by no more than 1%, as assessed by applying the data reduction scheme to flows with known conditions.

4.5. Validation measurements

As mentioned earlier, the interference probes listed in table 2 were tested in the turbulent region of the calibration jet, at a downstream distance of $x/D = 10$ from the jet exit. Validation measurements performed at this location are presented in figures 9 and 10 to demonstrate that an interference probe can be used to accurately measure velocity and helium concentration in turbulent flows. These results were measured with an interference probe consisting of a 5 μm diameter tungsten wire placed 10 μm upstream of a 2.5 μm diameter tungsten wire (more specifically, $l_{up} = 1.1$ mm, $l_{down} = 0.2$ mm, $OH_{up} = 1.8$, $OH_{down} = 1.2$). As may be observed from the one-dimensional longitudinal

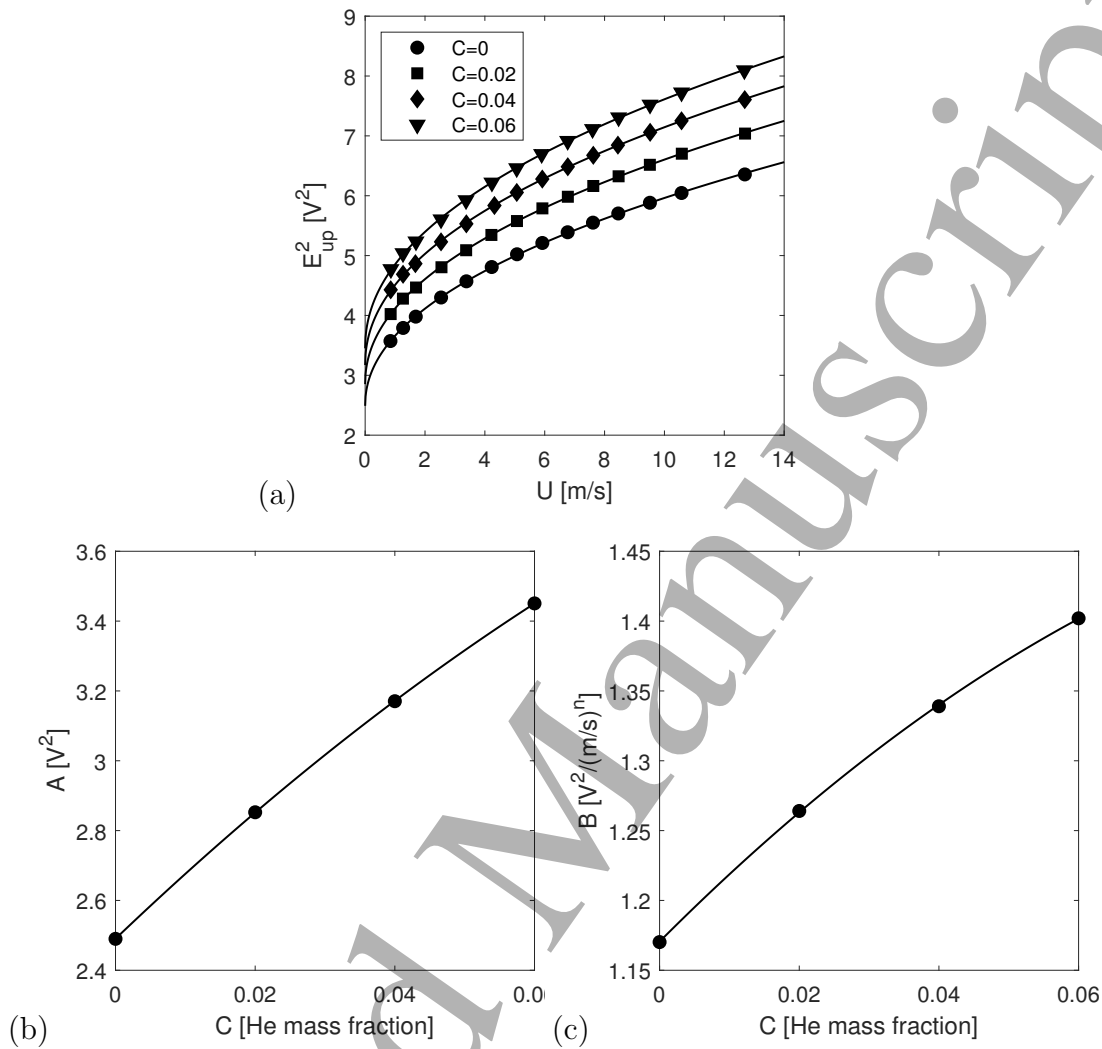*Thermal-anemometry-based probes to measure velocity and concentration* 17

(a)

(b)

(c)

Figure 8: (a) King's Law fits ($E^2 = A(C) + B(C)U^n$) of the upstream wire at 0, 0.02, 0.04, and 0.06 helium mass fractions. (b) Values of A calculated from the King's Law fits in (a) plotted as a function of C. (c) Values of B calculated from the King's Law fits in (a) plotted as a function of C. Both A and B are fit with second-order polynomials.

spectrum of velocity plotted in figure 9, the velocity measured by an interference probe agrees well with that measured by a single-normal hot-wire probe (a 5 μm diameter tungsten wire of the same length as the interference probe), for which the accuracy is already well established. Moreover, given that the velocity spectra measured by the two probes are very similar, it can be concluded that the frequency response of the interference probe is comparable to that a of conventional hot-wire-anemometry probe, at least over the range of frequencies measured, which extended up to 10 kHz. Similar results were reported by Sirivat and Warhaft [13] for their interference probe, which also consisted of two hot-wires (although their measurements were performed in grid turbulence at much lower frequencies).

In figure 10, the concentration spectrum measured in He/air mixtures is compared
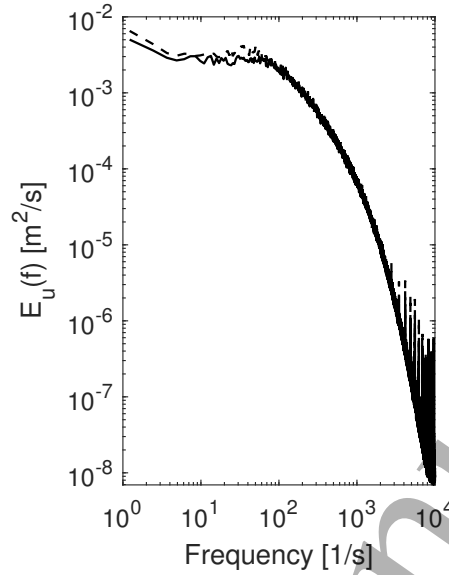
Thermal-anemometry-based probes to measure velocity and concentration   18

Figure 9: One-dimensional longitudinal velocity spectra measured in a turbulent jet of pure air with $Re_D = 4500$ using a single-normal hot-wire (- - - -) and an interference probe (——).
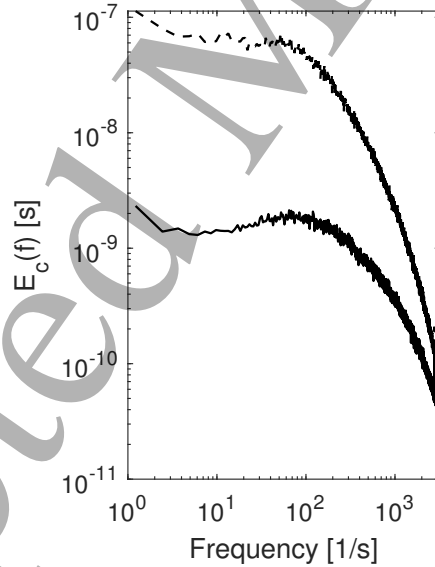

Figure 10: Concentration spectra measured using an interference probe in a turbulent jet of He/air (- - - -), where $C = 0.04$ at the jet exit and $Re_D = 3800$, and in a comparable jet of pure air (——). Note that although this data was measured with the same low pass frequency ($f_{LP} = 10$ kHz) and sampled at the same frequency ($2f_{LP}$) as the velocity data presented in figure 9, only measurements at frequencies up to 3200 Hz are depicted in this figure. Although f_{LP} approximates f_η (the Kolmogorov frequency), it is much larger than the analogous frequency for the scalar field ($f_{\eta_c} = \mathrm{Sc}^{3/4} f_\eta = 0.32 f_\eta \approx 0.32 f_{LP}$) due to the low Schmidt number of helium ($\mathrm{Sc} = 0.22$). Measurements at frequencies in the range $f_{\eta_c} < f < f_{LP}$ essentially consist of electronic noise, and are therefore not depicted.

Thermal-anemometry-based probes to measure velocity and concentration   19

with the concentration spectrum measured in pure air under the same nominal flow conditions. (The latter can be interpreted as the noise spectrum of the concentration measurements.) Although most interference probes investigated in the present work were found to adequately measure mean velocities and concentrations, the same was not always true for the fluctuating velocities and concentrations. The interference probe can exhibit spurious measurements of concentration in flows of pure air, similarly to what is observed when a cold-wire is operated in turbulent isothermal flows, where velocity fluctuations are misinterpreted as temperature fluctuations. In figure 10, the signal-to-noise ratio of the concentration measurements (SNR) is generally high, approaching two orders of magnitude at the lowest frequencies. However, as will be discussed in §4.6, this was not the case for many other interference probes developed for the present work. Despite designing probes with different diameter ratios, small separation distances ($< 50\,\mu$m), and different overheat ratios, the SNR remained poor for certain probe configurations, and it was difficult to accurately measure velocity and concentration fluctuations in turbulent flows. The experimental investigation presented in §4.6 therefore focuses on determining which design parameters can be used to create an interference probe with high SNR.

4.6. Effects of design parameters on the performance of an interference probe

The remainder of the probes presented in table 2 were analyzed similarly to the probe discussed in §4.5. Measurements were performed in (i) a turbulent jet of He and air, where $C = 0.04$ ($Re_D = 3800$), and (ii) a comparable jet of pure air. The quality of the measurements from each probe was quantified by calculating the signal-to-noise ratio of the concentration spectra in the limit as the frequency tends to 0 Hz (SNR_0):

$$SNR_0 = \lim_{f \to 0} E_c(f)/E_n(f), \tag{13}$$

where $E_c(f)$ and $E_n(f)$ are respectively the concentration spectrum measured in the He/air mixture and the noise spectrum measured in pure air. Given that (i) the largest scales (i.e. the smallest frequencies) contribute the most to the total scalar variance, and (ii) the highest frequencies ($f_{\eta_c} < f < f_{LP}$) primarily contain electronic noise (and thus should not be taken into account), SNR_0 was deemed a sensible measure of the signal-to-noise ratio.

The results of the analysis described above are plotted in figure 11. The first, and most important observation from this data is that the SNR does not improve as the diameter ratio increases. In fact, as can be observed in figure 11(a), the best results results are obtained when the diameter ratio is equal to 1. Note that this does not suggest that large SNR is correlated with small diameter ratios, since it is difficult to infer any trends in the data of figure 11(a) given that other parameters (separation distance, wire material) vary. The second important observation, gleaned from figure 11(b), is that in order to have high SNR, the separation distance between two wires should be very small; when normalized by the diameter of the upstream wire of the probe (which in the present work was always the hottest wire of the probe, so that $d_{up} = d_{hot}$), s/d_{up}

Thermal-anemometry-based probes to measure velocity and concentration   20

should be $\lesssim 2$, which agrees well with most previous work on this subject [4, 8, 10–14]. However, it should be emphasized that a small separation distance is not a sufficient condition for high SNR, as SNR_0 varied from 2.8 to 127 when $s/d_{up} \leq 2$.

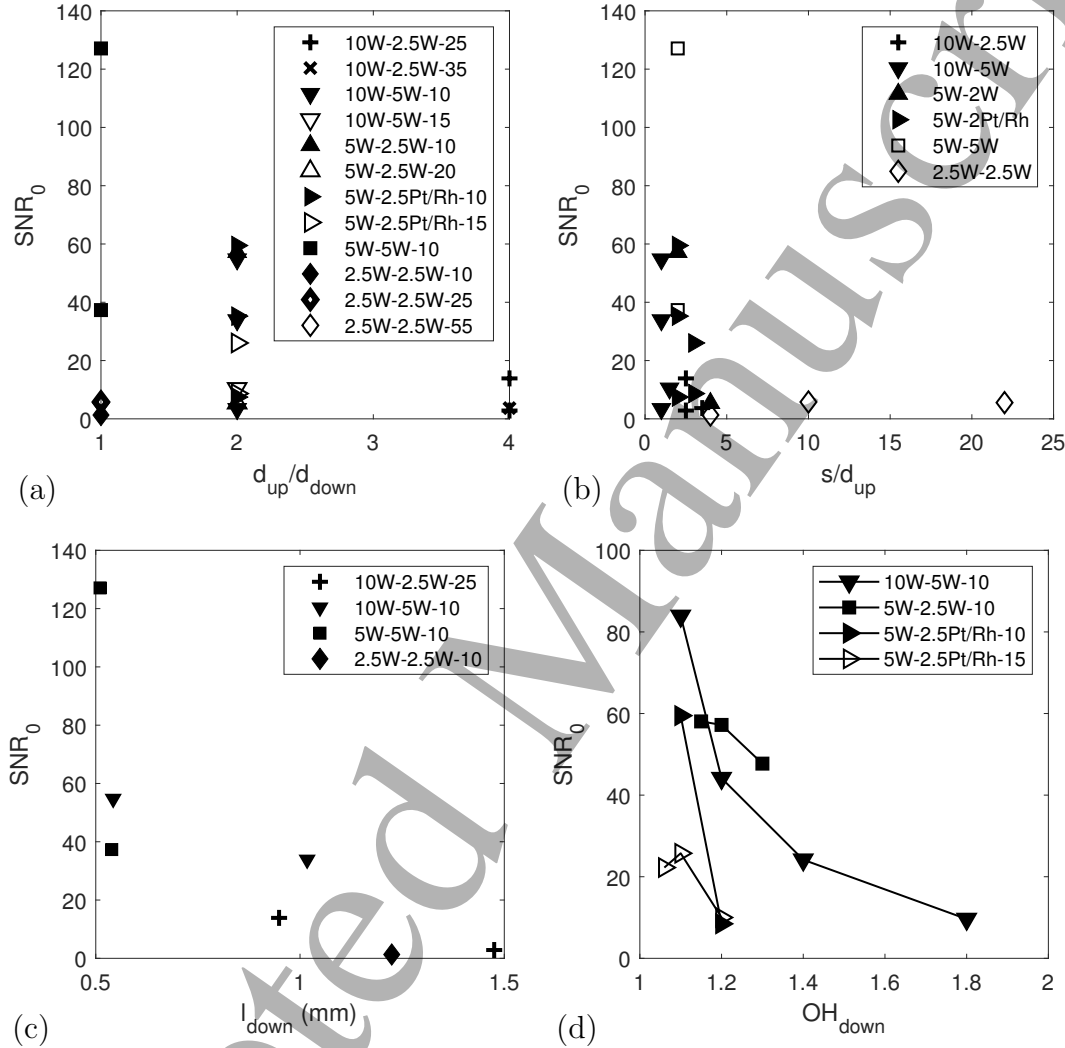Figure 11: SNR_0 of the interference probes listed in table 2 plotted as a function of the (a) diameter ratio (d_{up}/d_{down}), (b) separation distance normalized by the upstream wire diameter (s/d_{up}), (c) length of the downstream wire (l_{down}), and (d) overheat ratio of the downstream wire (OH_{down}). In (a), (b), and (c) the overheat ratios are kept constant as the parameter of interest is varied (1.8 for the upstream wire, and 1.2 or 1.1 for the downstream wire). In (d) the overheat ratio of the upstream wire is held constant at a value of 1.8.

The relationship between SNR_0 and the separation distance is further complicated by the fact that it is difficult to accurately measure the separation distance between the wires of the probe. This distance is only estimated with an accuracy of $\pm 5\,\mu$m *before* the wires of the probe are operated. Furthermore, when the wires are heated, they deflect away from each other, such that the actual separation distance may be larger than what is recorded. An example of the effect of heating on the separation distance of

Thermal-anemometry-based probes to measure velocity and concentration   21

the wires is shown in figure 12. Although it is not clear why the wires deflect away from each other, the fact that hot-wires may buckle when operated is known, and has been discussed by Perry [33]. To address this issue, the length of the downstream wire was reduced, as shorter wires will buckle less. The positive impact of the reduction of the downstream wire length is documented in figure 11(c), where it can be observed that SNR_0 is inversely related to the length of the downstream wire. It should be noted that using shorter downstream wires ($l_{down}/d_{down} < 200$) does not appear exacerbate end conduction effects or cause attenuation of turbulence measurements, as measurements from such probes were found to agree well with those from a single-normal hot-wire probe (e.g. figure 9).
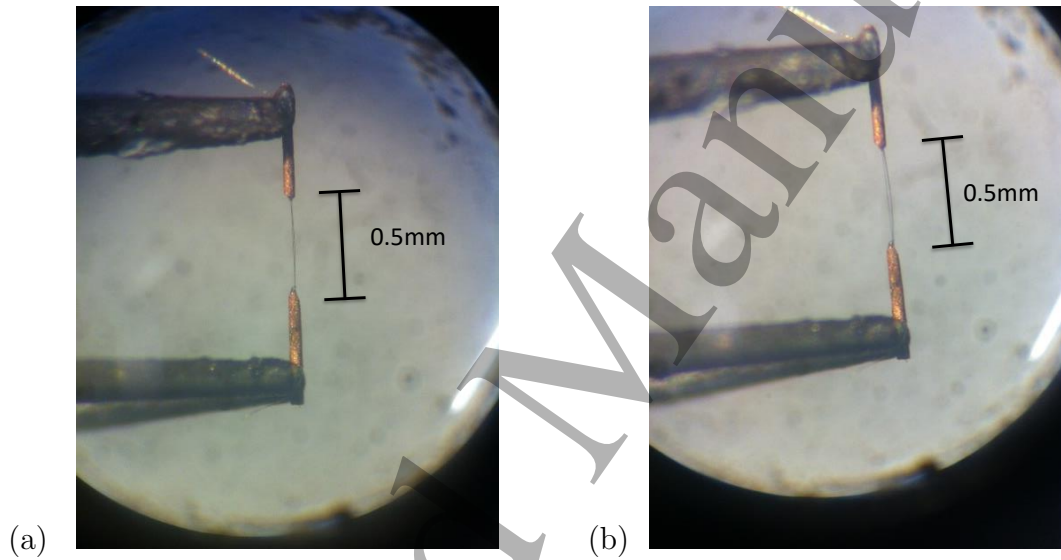

(a)   (b)

Figure 12: (a) Interference probe before the two wires are heated. The separation distance is measured to be $\lesssim 10\,\mu$m. (b) The same interference probe with both wires heated to approximately 220°C above the ambient temperature, depicting a larger separation distance.

One final point must be made regarding the design of interference probes. In §4.3, the choice of the overheat ratio for each wire was shown to have an impact on the shape of the calibration map. Further analysis shows that it also has an effect on the SNR. Figure 11(d) demonstrates that SNR_0 generally increases as the overheat ratio of the downstream wire is lowered while keeping the overheat ratio of the upstream wire constant. This is due to the fact that the wire is more sensitive to changes in fluid temperature (resulting from changes in the thermal wake of the upstream wire) when the overheat ratio (and thus the wire temperature) of the downstream wire is lowered. In some cases, diminishing returns from the effects of lowering the downstream wire overheat ratio may occur. This is likely because the voltage measured by the downstream wire decreases as the overheat ratio decreases (in some cases even approaching 0 if interference effects are too strong [5]), causing the wire to become more sensitive to electronic noise.

Thermal-anemometry-based probes to measure velocity and concentration   22

5. Conclusions and future work

The present work theoretically and experimentally analyzed how thermal-anemometry-based techniques can be used to simultaneously measure velocity and gas concentration in turbulent flows. Historically, the design of thermal-anemometry-based probes capable of making such measurements was based on the work of Corrsin [2,3] (and by extension, Harion et al. [5], Soudani et al. [6], and McQuaid and Wright [7]), who proposed using thermal-anemometry-based sensors of different diameters, and Way and Libby [4], who proposed having the sensors thermally interfere with each other. Although the use of different diameters may be supported in theory, this theory does not readily extend to flows containing helium, which is generally a popular gas for studying heterogeneous mixtures. Moreover, probes containing large diameter ratios are not practical; different hot-wires and/or hot-films are required, which may adversely affect the spatial and temporal resolution of the probe.

Herein, it is demonstrated that for a thermal-anemometry-based probe consisting of two hot-wires, the requirement of different diameters vanishes if the wires are placed close enough together that one is in the thermal field of the other. In addition to improving the temporal and spatial resolution of the probe, this greatly simplifies its design, since only one type of hot-wire is required. Thus, any system capable of making X-wire measurements can be adapted to making simultaneous velocity and concentration measurements. We show that the aforementioned thermal-anemometry-based probes (i.e. interference probes) can be used to make simultaneous measurements of velocity and helium concentration in turbulent flows and that their performance is improved when (i) the normalized wire separation distance (s/d_{up}) is below 2, and (ii) the downstream wire overheat ratio is low. To ensure the separation distance between the wires remains sufficiently small while they are operated, a short downstream wire is also recommended.

It is important to note that interference probes behave similarly to single-normal hot-wires; they have comparable accuracies, frequency responses, spatial resolutions, and, also, comparable limitations. For example, an interference probe only measures a single component of velocity, and must be combined with other thermal-anemometry-based sensors (hot-wires, hot-films) to measure additional components of the velocity field [10–12, 14]. Moreover, for any researchers seeking to use these probes, it should be emphasized that the design recommendations herein were based on experiments performed in isothermal He/air mixtures, where $0 \leq C \leq 0.06$. At higher helium concentrations, certain adjustments – perhaps to the wire overheat ratios – may be necessary to ensure that the effects of thermal interference are not too strong (as this could cause the voltage measured across the downstream wire to approach 0). To use these probes in other gas mixtures, or in non-isothermal flows, further work is required. Development of a temperature compensation method for interference probes is currently underway.

Thermal-anemometry-based probes to measure velocity and concentration   23

Acknowledgments

Appendix A. Nomenclature

A, B	numerical constants
a, b	numerical constant
C	concentration, He mass fraction
c_i	numerical constants
D	diameter of jet
d	diameter of wire
E	anemometer output voltage
E_c	concentration spectrum
E_n	noise spectrum
E_u	velocity spectrum
E_w	wire voltage
f	frequency
f_{LP}	low-pass frequency
f_η	maximum frequency of velocity field / Kolmogorov frequency
f_{η_c}	maximum frequency of scalar field
h	heat transfer coefficient of wire
h_S	heat transfer coefficient of wire at T_S in perfectly continuous gas
I	current through wire
k	thermal conductivity of fluid
Kn	Knudsen number
l	length of wire
n	numerical constant (exponent in King's Law)
Nu	Nusselt number
Nu_c	continuum Nusselt number
OH	overheat ratio ($\equiv R_w/R_a$) of wire
Pr	Prandtl number
q''	heat flux from wire
R_{20}	resistance of wire at 20°C
R_a	cold-resistance of wire
R_L	total cable resistance
R_T	top-resistance of the Wheatstone bridge of a CTA
R_w	resistance of wire (while being operated)
r	cylindrical coordinate
Re	Reynolds number
s	separation distance
Sc	Schmidt number
T	temperature of the fluid
T_f	film temperature ($\equiv \frac{Tw+T}{2}$) of wire
T_S	extrapolated wire temperature
T_w	temperature of wire
U	velocity of the fluid
X	mole fraction of helium
x	cylindrical coordinate

Thermal-anemometry-based probes to measure velocity and concentration 24

α accommodation coefficient

α_{20} temperature coefficient of resistivity of wire at 20˚C

β slip parameter

γ ratio of specific heats

Δ temperature jump distance

λ mean free path

μ dynamic viscosity of fluid

Φ parameter quantifying accommodation effects

ρ density of fluid

Other subscripts

1   wire 1

2   wire 2

air   in air

down   downstream wire

F   hot-film

hot   denoting the hottest sensor of a probe

He   in helium

T_S at temperature T_S

T_w at temperature T_w

up   upstream wire

W   hot-wire

Appendix B. Derivation of equation (1)

For a long hot-wire ($l/d > 200$) operated at a constant temperature, both heat transfer by radiation and conduction can be assumed to be negligible, such that the heat generated by passing an electric current through the wire is effectively equal to the heat convected away by the fluid flow:

$$I^2 R_w = h\pi d l (T_w - T). \tag{B.1}$$

Given that the temperature of the wire can be related to its resistance by the following relation [1]:

$$R_w = R_{20}[1 + \alpha_{20}(T_w - T_{20})], \tag{B.2}$$

and using the convective heat transfer correlation for a long cylinder developed by Collis and Williams [22]:

$$\text{Nu}_c \left(\frac{T_f}{T}\right)^{-0.17} = 0.24 + 0.56\text{Re}^{0.45}, \tag{B.3}$$

equation (B.1) can be re-expressed as:

$$\frac{E_w^2}{R_w} = \pi l k \left(\frac{R_w - R_a}{\alpha_{20}R_{20}}\right)\left(\frac{T_f}{T}\right)^{0.17}(0.24 + 0.56\text{Re}^{0.45}). \tag{B.4}$$

To account for assumptions in the derivation of equation (B.4), such as, for example, end conduction effects, the Reynolds number exponent (0.45) is replaced by a

Thermal-anemometry-based probes to measure velocity and concentration   25

variable, denoted as n. Additionally, given that experimentalists typically measure the anemometer bride voltage (E) (see Hewes et al. [32]) :

$$E = \frac{R_T + R_L + R_w}{R_w} E_w, \tag{B.5}$$

equation (B.4) can be re-written as:

$$E^2 = \pi l k \left(\frac{R_w - R_a}{\alpha_{20} R_{20}} \right) \frac{(R_T + R_L + R_w)^2}{R_w} \left(\frac{T_f}{T} \right)^{0.17}$$
$$\left[0.24 + 0.56 \left(\frac{\rho U d}{\mu} \right)^n \right] = A + B U^n. \tag{B.6}$$

If the overheat ratio ($OH \equiv R_w/R_a$) is assumed to be constant, equation (B.6) can be used to obtain equations (2) and (3). Note that all fluid properties are evaluated at the film temperature of the wire (T_f). Additionally, in He/air mixtures, $\rho = (1 - X)\rho_{air} + X\rho_{He}$ (where X is the mole fraction of helium), and μ and k are respectively evaluated using expressions derived by Wilke [34] and Mason and Saxena [35].

Appendix C. Derivation of equation (10)

As per the work of Collis and Williams [22], Andrews et al. [23], and Kennard [36], the temperature discontinuity at the heated surface of a hot-wire (temperature T_w) undergoing thermal slip can be expressed as follows:

$$T_w - T_S = -\Delta \frac{\partial T}{\partial r}, \tag{C.1}$$

where T_S is the value of the fluid temperature that would occur if $\partial T/\partial r$ remained unchanged up to the wire surface, and Δ is the "temperature jump distance":

$$\Delta = \left(\frac{2 - \alpha}{\alpha} \right) \left(\frac{2\gamma}{\gamma + 1} \right) \left(\frac{\lambda}{\mathrm{Pr}} \right). \tag{C.2}$$

Given that the actual rate of heat transfer from a hot-wire at temperature T_w is assumed to be equal to the rate of heat transfer from the same wire at temperature T_S in a perfectly continuous gas, such that:

$$q'' = h_w(T_w - T) = h_S(T_S - T); \tag{C.3}$$

and that the heat flux (q'') is also equal to:

$$q'' = -k_{T_S} \left(\frac{\partial T}{\partial r} \right)_{T_S}, \tag{C.4}$$

the continuum Nusselt number ($\mathrm{Nu}_c \equiv h_S d/k$) can be expressed in terms of the actual Nusselt number ($\mathrm{Nu} \equiv h_w d/k$) as follows:

$$\mathrm{Nu}_c = \mathrm{Nu} \left(1 + \frac{\mathrm{Nu}_c \Delta_{T_s} k}{k_{T_s} d} \right). \tag{C.5}$$

Equation (C.5) can be re-arranged to yield:

$$\mathrm{Nu}_c = \frac{\mathrm{Nu}}{1 - \mathrm{Nu} \Phi \mathrm{Kn}}, \tag{C.6}$$

Thermal-anemometry-based probes to measure velocity and concentration 26

where $\Phi = f(\alpha)$, as seen below:

$$\Phi = \left(\frac{\Delta_{T_S}}{d\mathrm{Kn}_{T_S}}\right)\left(\frac{\mathrm{Kn}_{T_S}}{\mathrm{Kn}}\right)\left(\frac{k}{k_{T_S}}\right) =$$
$$\left(\frac{2-\alpha}{\alpha}\right)\left(\frac{2\gamma}{\gamma+1}\right)\left(\frac{1}{\mathrm{Pr}_{T_S}}\right)\left(\frac{\mathrm{Kn}_{T_S}}{\mathrm{Kn}}\right)\left(\frac{k}{k_{T_S}}\right), \quad (C.7)$$

and assuming T_S is reasonably close to T_w [23, 27], can be approximated as follows:

$$\Phi \approx \left(\frac{2-\alpha}{\alpha}\right)\left(\frac{2\gamma}{\gamma+1}\right)\left(\frac{1}{\mathrm{Pr}_{T_w}}\right)\left(\frac{\mathrm{Kn}_{T_w}}{\mathrm{Kn}}\right)\left(\frac{k}{k_{T_w}}\right). \quad (C.8)$$

Since the heat transfer correlation of Collis and Williams [22] is only valid for continuum flows, when rarified gas and accommodation effects are present, equations (C.6) and (C.7 or C.8) must be combined with equation (B.3) to obtain the actual convective heat transfer correlation for the hot-wire. If equation (B.6) is re-derived using the actual heat transfer correlation, this yields equation (10).

To use equation (10) in He/air mixtures, as we have done in §3.2, the accommodation coefficient in these mixtures must be estimated. Based on the literature, one can assume that $\alpha_{air} = 1$ and $\alpha_{He} = 0.48$ [27]. However, there is very little information on values of α in gas-mixtures (and more specifically, He/air mixtures). Using data provided by Wu and Libby [26], we assume that the slip parameter β:

$$\beta = \frac{\Delta}{d} = \left(\frac{2-\alpha}{\alpha}\right)\left(\frac{2\gamma}{\gamma+1}\right)\left(\frac{\mathrm{Kn}}{\mathrm{Pr}}\right) \quad (C.9)$$

in He/air mixtures can be expressed as a linear function of its pure components (β_{air}, β_{He}), as shown below:

$$\beta = \beta_{He}C + \beta_{air}(1-C). \quad (C.10)$$

It should be noted that Wu and Libby [26] suggested that $\beta = X\beta_{He}$, where X is the mole fraction of helium. However, from inspection of their data, equation (C.10) appears to be a more appropriate choice. Moreover, the expression suggested by Wu and Libby [26] predicts that $\beta = 0$ in pure air, which yields an unrealistic value of α.

References

[1] Bruun H 1995 *Hot-wire Anemometry: Principles and Signal Analysis* (Oxford University Press)
[2] Corrsin S 1947 *Rev. Sci. Instr.* **18** 469–471
[3] Corrsin S 1949 Extended application of the hot-wire anemometer Tech. Note 1864 NACA
[4] Way J and Libby P 1970 *AIAA J.* **8** 976–978
[5] Harion J L, Favre-Marinet M and Camano B 1996 *Exp. Fluids* **22** 174–182
[6] Soudani A, Bougoul S and Harion J L 2002 *Rev. Energ. Ren.* 75–92
[7] McQuaid J and Wright W 1973 *Intl. J. Heat Mass Transfer* **16** 819–828
[8] Way J and Libby P 1971 *AIAA J.* **9** 1567–1573
[9] McQuaid J and Wright W 1974 *Intl. J. Heat Mass Transfer* **17** 341–349
[10] Stanford R A and Libby P 1974 *Phys. Fluids* **17** 1353
[11] LaRue J and Libby P 1977 *Phys. Fluids* **20** 192–202

Thermal-anemometry-based probes to measure velocity and concentration   27

[12] LaRue J and Libby P 1980 *Phys. Fluids* **23** 1111–1118

[13] Sirivat A and Warhaft Z 1982 *J. Fluid Mech.* **120** 475

[14] Panchapakesan N and Lumley J 1993 *J. Fluid Mech.* **246** 225

[15] Riva R, Binder G, Favre-Marinet M and Harion J L 1994 *Exp. Therm. Fluid Sci.* **9** 165–173

[16] Harion J L, Favre-Marinet M and Binder G 1997 *Exp. Therm. Fluid Sci.* **14** 92–100

[17] Soudani A and Bessaïh R 2004 *Acta Mech.* **171** 225–240

[18] Soudani A and Bessaïh R 2006 *Acta Mech.* **181** 207–229

[19] Sakai Y, Watanabe T, Kamohara S, Kushida T and Nakamura I 2001 *Int. J. Heat Fluid Fl.* **22** 227–236

[20] Jonáš P, Mazur O, Šarboch J and Uruba V 2003 *Proc. Appl. Math. Mech.* **3** 356–357

[21] Mazur O, Jonáš P, Šarboch J and Uruba V 2003 *Proc. Appl. Math. Mech.* **2** 336–337

[22] Collis D and Williams M 1959 *J. Fluid Mech.* **6** 357–384

[23] Andrews G, Bradley D and Hundy G 1972 *Intl. J. Heat Mass Tranfer* **15** 1765–1786

[24] Kassoy D 1967 *Phys. Fluids* **10** 938

[25] Aihara Y 1967 *Phys. Fluids* **10** 947

[26] Wu P and Libby P 1971 *Int. J. Heat Mass Transfer* **14** 1071–1077

[27] Pitts W M and McCaffrey B J 1986 *J. Fluid Mech.* **169** 465–512

[28] Hewes A 2016 *Development of an interference probe for the simultaneous measurement of turbulent concentration and velocity fields* Master's thesis McGill University

[29] Hewes A 2020 *Multi-scalar mixing in turbulent coaxial jets* Ph.D. thesis McGill University

[30] Berajeklian A 2010 *Simultaneous measurements of velocity and temperature in the heated wake of a cylinder with applications to the modeling of turbulent passive scalars* Master's thesis McGill University

[31] Berajeklian A and Mydlarski L 2011 *Phys. Fluids* **23** 055107

[32] Hewes A, Medvescek J I, Mydlarski L and Baliga B R 2020 *Meas. Sci. Technol.* **31** 045302

[33] Perry A 1982 *Hot-wire anemometry* (Clarendon Press)

[34] Wilke C 1950 *J. Chem. Phys.* **18** 517

[35] Mason E and Saxena S 1958 *Phys. Fluids* **1** 361–369

[36] Kennard E H 1938 *Kinetic Theory of Gases* (McGraw-Hill)